Jestr

Journal of Engineering Science and Technology Review 15 (6) (2022) 170 - 177

JOURNAL OF
Engineering Science and Technology Review

Research Article

www.jestr.org

Influence Factors Analysis of Projectile Kinetic Energy at Muzzle of Magnetoresistive Coil Gun

Jian Gong[1], Dalu Fang[1], Weimin Liang[1,*] and Shuren Wang[1,2]

[1] *School of Civil Engineering, Henan Polytechnic University, Jiaozuo 454003, China*
[2]*International Joint Research Laboratory of Henan Province for Underground Space Development and Disaster Prevention, Henan Polytechnic University, Jiaozuo 454003, China*

Received 23 September 2022; Accepted 15 December 2022

Abstract

The kinetic energy at the muzzle of a magnetoresistive coil gun is an important parameter for gun optimization. It is of significance to study the influence of parameters such as coil inductance, energy storage capacitance, discharge voltage and the relative position of the projectile in the coil on the projectile kinetic energy at the muzzle. The formula for the muzzle kinetic energy of the coil gun projectile was obtained by MATLAB function fitting. The correlation coefficients between the muzzle kinetic energy and coil inductance, energy storage capacitance, discharge voltage and the projectile's relative position in the coil were calculated by SPSS software, respectively. Results show that the error between the projectile kinetic energy at the muzzle measured through verification experiment and that calculated by the formula is less than 10%, indicating the reliability of the fitting formula. The coil inductance, energy storage capacitor, discharge voltage and the relative position of the projectile in the coil influence the projectile kinetic energy at the muzzle in different degrees, with the correlation coefficients |r| being 0.301, 0.518, 0.442 and 0.17, respectively. The conclusions obtained in this study provide the reference increasing the kinetic energy of the bullet at the muzzle of magnetoresistive coil gun.

Keywords: Magnetoresistive coil gun, Projectile kinetic energy, Multivariate function fitting, correlation coefficient

1. Introduction

Magnetoresistive coil gun is a device that converts electromagnetic energy into kinetic energy. Compared with traditional launchers, it can propel an object to extremely high speeds in a very short period of time. With its advantages over conventional launch technology, such as large thrust, ease in control, long service life and the ability to improve projectile velocity without loading gunpowder, the magnetoresistive coil gun has attracted investments all over the world [1].

Conceptually, there is no limit to the movement of objects in an electromagnetic field. Over the last 30 years, different shapes of electromagnetic launchers have been developed for use in low and medium speed rocket launchers, long-range and high-speed launchers, space systems and impact and vibration testing machines [2-5], etc.

Compared with the engineering applications, the theoretical research of magnetoresistive coil gun was slow. Due to the numerous factors affecting the electromagnetic force and the mutual influence among them, and the insufficient calculation accuracy of the electromagnetic field in high-speed environment, the theoretical research is faced with a lot of difficulties. In the process of projectile launching, the circuit has a high voltage, large current and low energy utilization rate, so the acceleration effect of the projectile cannot be fully utilized. The muzzle velocity of the projectile and the power utilization efficiency of the system are important indexes for evaluating the performance of the electromagnetic launcher. Therefore, many scholars have conducted in-depth research on the the factors affecting the muzzle velocity and the new technologies to improve the muzzle velocity.

2. State of the art

It has gained growing attention to increase projectile kinetic energy at muzzle of the magnetoresistive coil gun [6-9]. For the launch process, simulation is one of the important means. Xiang et al. established the mathematical model of coil gun firing and introduced its working mechanism [10, 11]. Niu et al. established the coil heating model and studied the relationship between the temperature and different structural parameters and the coil gun acceleration [12]. Zhang et al. established the coil gun firing model by Ansys software and they obtained the relationship between the material, length, position and shape of the projectile and the muzzle velocity of the coil gun, respectively [13, 14]. Guo & Su simulated and analyzed the relationship between the drive coil length and optimal trigger position and the muzzle velocity of the projectile [15]. Orbach et al. optimized the structural parameters of the single-stage coil gun by the experimental and numerical simulations [16, 17]. Guan et al. studied the circuit system and solved the problem of field-circuit coupling analysis when the coilgun was powered by pulses [18, 19]. Kim & Kim optimized the projectile by analyzing its resistance coefficient and they verified its performance through experiments [20].

Current research on coil gun is mainly focused on simulation and circuit system, with the structural parameters and circuit parameters of the drive coil studied respectively.

*E-mail address: liangwmhpu@126.com
ISSN: 1791-2377 © 2022 School of Science, IHU. All rights reserved.
doi:10.25103/jestr.156.21

However, the material and mass of the projectile also have a certain impact on the muzzle velocity. Coramik et al. designed a coilgun in which a stator optical system was inserted on the projectile to measure its speed. They obtained the real-time data for each launch through the detector, and accordingly changed the variables such as coil voltage, coil length and trigger point, so that the projectile could reach a higher speed at leaving the muzzle [21]. He & wang studied the projectile velocity under different voltages and drew the conclusion that the muzzle velocity increased with the increase of voltage [22]. Ranashree & Thomas studied different sizes of aluminum projectiles and anlyzed the muzzle velocities at different initial positions and under varying charging voltages [23].

Since there are few studies on the correlation among the projectile parameters, drive coil parameters and circuit parameters of the magnetoresistive coil gun, in this study, the relationship between the projectile kinetic energy at muzzle and the coil inductance, energy storage capacitance, discharge voltage and the relative position of the projectile was studied from the perspective of energy, so as to reduce the error caused by the mass of the projectile and other factors. MATLAB software was used to fit the functional relationship between the projectile kinetic energy at muzzle and the four variables aforementioned, and the fitting results were verified through verification experiments. SPSS software was used for correlation analysis to study the degree of correlation between the four variables and the projectile kinetic energy at muzzle, with the aim to improve the muzzle kinetic energy of the coil gun and optimize the drive coil structure.

The rest of this study is organized as follows. Section 3 presents the working mechanism of coil gun and experimental design. Section 4 gives the results analysis and discussion, and finally, the conclusions are summarized in Section 5.

3. Methodology

3.1 Working mechanism of coil gun

The magnetoresistive coil gun works by driving the accelerated movement of the projectile through the electromagnetic force generated from the interaction between the magnetic field produced by the changing current in the energized coil and the induced eddy current of the projectile. Its working process is complex, involving electrical, magnetic and mechanical movements, and which is subjected to various factors. For easier analysis, the following assumption is made as follows: the air resistance of the projectile, the inherent resistance and inductance in the loop (including capacitor inductance, discharge switch inductance and lead inductance) and the influence of the device for securing the drive coil on the structure are ignored. Fig. 1 shows the simplified equivalent circuit.

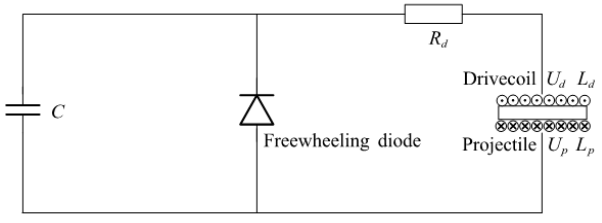

Fig. 1. Equivalent circuit diagram.

U_0, U_d and U_P are the initial voltage of the capacitor, the voltage of the drive coil and the induced voltage of the projectile, respectively. L_d and L_P are the inductance of the drive coil and the total inductance of the projectile. R_d and R_P are the total resistance of the discharge loop and the total resistance of the projectile. i_d and i_p are the current generated by the drive coil and the projectile and the current generated by the energized drive coil. v_p represents projectile velocity. m is projectile mass. M is the mutual inductance between the drive coil and the projectile, which is a function of the projectile position x [24, 25].

The circuit equations are as follows:

$$U_\mathrm{d} = i_d R_d + L_d \frac{d_{id}}{dt} + L_d \frac{d_{id}}{dt} - \frac{M d_{ip}}{dt} - v_p \frac{dM}{dx} i_\mathrm{p} \tag{1}$$

$$U_\mathrm{p} = i_p R_p + L_p \frac{d_{ip}}{dt} + L_p \frac{d_{ip}}{dt} - \frac{M d_{id}}{dt} - v_p \frac{dM}{dx} i_d \tag{2}$$

The kinematic equations are as below:

$$a = \frac{1}{m} \frac{dM}{dx} i_p i_d \tag{3}$$

$$v = at \tag{4}$$

By combining the equations above, it can be seen that the kinetic energy of the projectile is not only related to the energy storage capacity of the capacitor, the driving structure and the projectile material, but also related to the starting position of the projectile and its length into the drive coil.

3.2 Experimental design

The coil gun is composed of a charge loop, a discharge loop and a drive coil. The charge loop is mainly composed of power supply, transformer, charge switch and energy storage capacitor. The discharge loop is mainly composed of energy storage capacitor, discharge switch, freewheeling diode (FWD), drive coil and projectile.

Drive coils with different inductances were obtained by winding the enamelled wires of different diameters into coils with different layers and lengths. The FWD was connected in parallel at both ends of the drive coil to form a closed loop to avoid capacitor breakdown or burnout caused by the induced high-voltage after discharge. The transformer adopted the DC-DC high voltage booster module, with an input voltage of 8-32 V and an output voltage continuously adjustable in the range of ±45-780 V.

The capacitance was measured by the multimeter. Due to the measurement conditions, instruments and capacitor aging, the measured value was about 800 μF, which was lower than the standard value. The following experiments were conducted based on the measured values. Table 1 shows the component parameters required by the circuit.

The high-speed camera (PMM-310) with the supporting PCC photography control software camera is shown in Fig. 2. The camera was connected with the computer through gigabit network cable, and fast-moving objects were captured by adjusting the camera resolution, frame rate, exposure time and other parameters. The speed of the object could be obtained through conversion.

Table 1. The computational parameters

Name	Attribute	Quantity
DC regulated power supply	0-220 V continuously adjustable	1
Capacitance	450 V, 1000 μF	20
DC-DC high voltage booster module	±45-390 V 780 V	1
Diode	200 A, 1600 V	2
Enameled wire	Copper wire with diameters of 1.08 mm, 1.20 mm and 1.60 mm	25 kg
Projectile	Diameter 10 mm, length 100 mm and mass 0.6 kg	1

Fig. 2. High speed camera.

Fig. 3 is the simplified charge/discharge circuit and Fig. 4 is the picture of the charge/discharge unit. The specific experimental procedures were as follows: The unit was powered on, adjusting the voltage (adjustable from 0-780 V) through the transformer to the required value. The charge switch was closed to charge the capacitor. After the charging being completed, the charge switch was disconnected, closing the discharge switch, and the projectile was shot out of the gun tube. All electrical components in the charge/discharge unit had an influence on the muzzle kinetic energy of the projectile in idfferent degrees, especially the characteristics of the drive coil, the parameters of the charge/discharge circuit module and the position of the projectile. In the following sections, the tests were carried out to study the influence of coil inductance L, discharge voltage U, energy storage capacitance C and relative position S of the projectile on the projectile's kinetic energy E at muzzle.

3.2.1 Coil inductance on kinetic energy at muzzle

When an alternating current (AC) was passing through a wire, alternating magnetic flux was generated in and around the wire. Inductance was defined as the ratio of the magnetic flux to the current causing it and an important index for coil performance. As the intrinsic characteristic of the coil, the inductance had nothing to do with the current intensity. It is mainly affected by the number of turns, size, shape, winding mode and core material of the coil. The analytical formula of inductance can be obtained with the energy method [26]:

$$L = 2\pi\mu_0 \frac{N^2 R_1^5}{(R_2 - R_1)^2 D^2} T(p,q) \quad (5)$$

where, D is the length of the coil. N is the number of turns. R_1 the inner diameter, and R_2 is the outer diameter of the coil. $\mu_0 = 4\pi\times10^{-7}$ H/m, $T(p,q)$ is the functional of the Bessel function of the first kind.

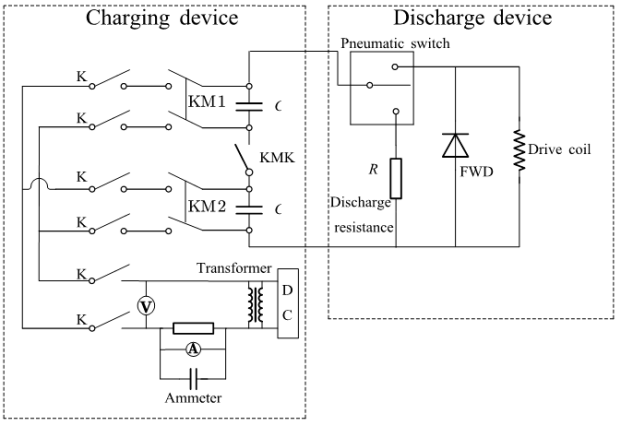

Fig. 3 Charge/discharge circuit.

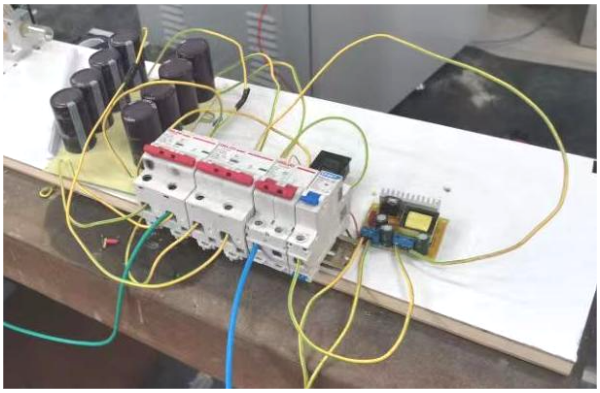

Fig. 4. Picture of charge/discharge unit.

As shown in Fig. 5, the coils (innder diameter 17 mm) with different turns and lengths were prepared and the inductance values were calculated. Table 2 lists the inductance and related parameters of each coil.

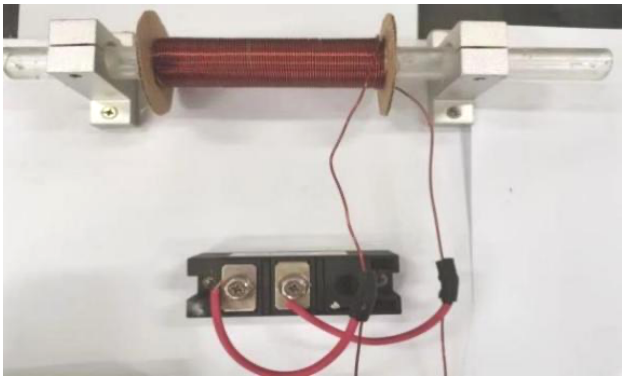

Fig. 5. Drive coil.

Table 2. Coil parameters.

Outer diameter (mm)	Number of turns N	Length l (mm)	Inductance L (H)
20.0	82	100	0.16
27.0	323	100	2.80
31.6	485	100	23.93
39.8	726	100	15.19
40.9	808	100	54.49
27.0	202	60	1.98
27.0	484	150	4.18

3.2.2 Voltage on kinetic energy at muzzle

A 100 mm-long coil was prepared by winding four layers of 1.08 mm enamelled wire. The outer diameter of the coil was 27 mm, the number of turns 323, the inductance 2.798 H, the capacitance capacity 1600 μF and the projectile position 0.5.

The projectile kinetic energy at muzzle was measured by adjusting the charging voltage via the booster module.

3.2.3 Capacitance on projectile kinetic energy at muzzle

A 100 mm-long coil was prepared by winding four layers of 1.08 mm enamelled wire. The outer diameter of the coil was 27 mm, the number of turns 323, the inductance 2.80 H, the voltage set to 660 V, and the projectile position 0.5. The capacitance was changed by changing the number of series and parallel capacitors, and on this basis, the projectile kinetic energy at muzzle was calculated by a high-speed camera.

3.2.4 Projectile position on projectile kinetic energy at muzzle

A 100 mm-long coil was prepared by winding four layers of 1.08 mm enamelled wire. The outer diameter of the coil was 27 mm, the number of turns 323, the inductance 6797.98 μH, the voltage 660 V and the capacitance 2000 μF. By changing the initial position of the projectile, its kinetic energy at muzzle was calculated by the high-speed camera.

4. Results analysis and discussion

4.1 Influence analysis of coil inductance on projectile kinetic energy at muzzle

With the voltage increased to 660 V by adjusting the booster module, the capacitance capacity being 1600 μF and the relative position of the projectile being 0.5 (half length of the projectile was put into the coil), the relationship between the coil inductance and the projectile kinetic energy at muzzle was studied. The muzzle velocity of the projectile was calculated using the high-speed camera, which was then converted into its kinetic energy at muzzle, as shown in Table 3. The relationship between the inductance and the kinetic energy at muzzle (velocity) fitted by Origin is shown in Fig. 6.

Table 3. Relationship between coil inductance and projectile kinetic energy at muzzle.

Inductance *L* (H)	Velocity *v* (m/s)	Kinetic energy at muzzle *E* (J)
0.16	2.65	0.21
1.98	7.72	1.77
2.78	9.45	2.64
4.19	12.67	4.74
15.19	14.81	6.49
23.93	12.45	5.59
30.92	14.07	5.86
40.57	11.51	3.92
54.49	16.38	3.19

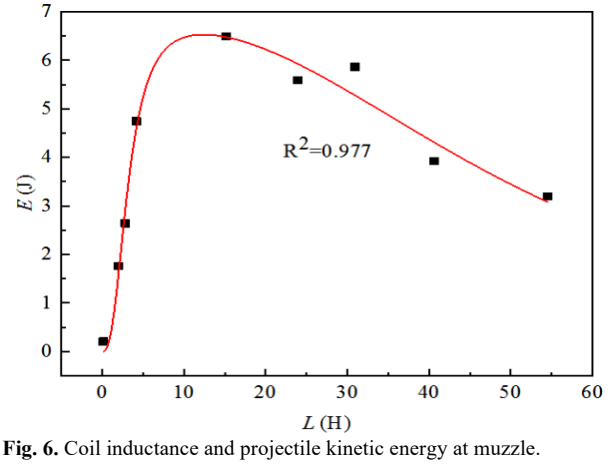

Fig. 6. Coil inductance and projectile kinetic energy at muzzle.

As can be seen from Fig. 6, the projectile kinetic energy at muzzle increases first and then decreases with the increase of inductance. When the inductance is 15.192 H, the kinetic energy reaches a maximum of 6.492 J and the velocity reaches 14.810 m/s. When the inductance is greater than 15.19 H, the projectile kinetic energy at muzzle starts to decrease. Therefore, it is not a wise choice to keep increasing the inductance to get a higher projectile kinetic energy at muzzle.

4.2 Influence analysis of voltage on projectile kinetic energy at muzzle

The measured kinetic energy at muzzle is shown in Table 4. The relationship between voltage and kinetic energy at muzzle fitted by Origin is shown in Fig. 7.

Table 4. Relationship between voltage and projectile kinetic energy at muzzle.

Voltage *U* (V)	Velocity *v* (m/s)	Energy *E* (J)
100	1.54	0.07
200	3.91	0.45
300	6.15	1.13
400	7.68	1.75
500	9.95	2.93
600	11.53	3.93
700	12.30	4.48

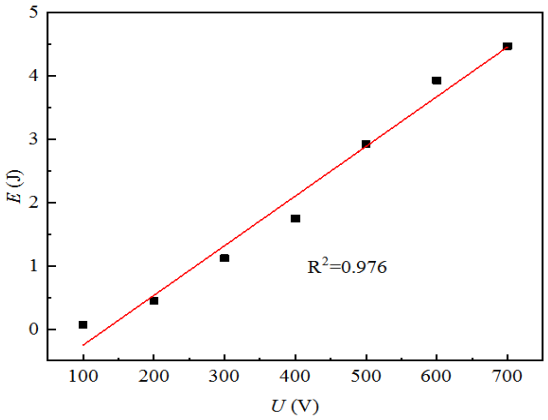

Fig. 7. Relationship between voltage and projectile kinetic energy at muzzle.

As seen from Fig. 7, the projectile kinetic energy at muzzle increases linearly with the voltage. The unit can accelerate the projectile to 12.30 m/s at a voltage of 700 V, which converts into a kinetic energy of 4.48 J. Therefore, to get a greater kinetic energy at muzzle, we can increase the voltage as long as it is safe to do so.

4.3 Influence analysis of capacitance on projectile kinetic energy at muzzle

The projectile kinetic energy values at muzzle calculated by the high-speed camera are shown in Table 5. The relationship between the capacitance and the kinetic energy fitted by Origin is shown in Fig. 8.

Table 5. Relationship between projectile kinetic energy at muzzle and capacitance.

Capacitance *C* (μF)	Velocity *v* (m/s)	Energy *E* (J)
400	2.73	0.22
800	5.10	0.77
1200	7.46	1.65
1600	12.88	4.91
2000	14.01	5.81

2400	14.29	6.04
2800	15.23	6.86
3200	16.24	7.80
3600	14.50	6.22
4000	14.46	6.19
4400	14.32	6.07
4800	14.43	6.16

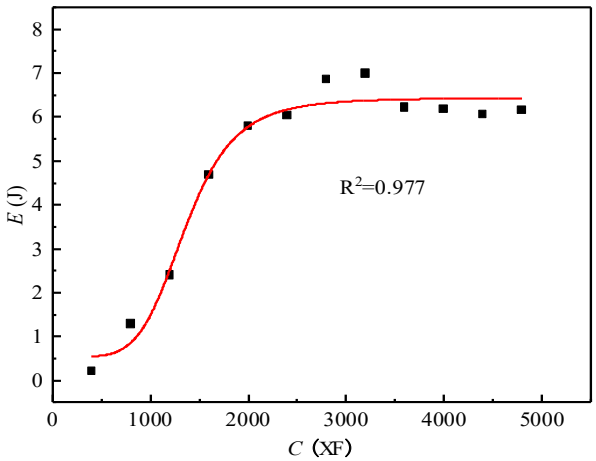

Fig. 8. Relationship between capacitance and projectile kinetic energy at muzzle.

It can be found from the Fig. 8 that when the capacitance is 0-3200 μF, the projectile kinetic energy at muzzle increases with the increase of capacitance. At 3200 μF, when the discharge voltage is 660 V, the projectile kinetic energy at muzzle reaches up to 7.8 J. When the capacitance is greater than 3200 μF, the projectile kinetic energy at muzzle tends to be stable instead of changing with the increase of capacitance. That is, when the capacitance grows to a certain level, it is no longer a strong driver for the increase of the projectile kinetic energy at muzzle.

4.4 Influence analysis of projectile position on projectile kinetic energy at muzzle

The projectile kinetic energy values at muzzle calculated by the high-speed camera are shown in Table 6. The relationship between the relative position of the projectile and the kinetic energy fitted by Origin is shown in Fig. 9.

Table 6. Relationship between relative position of projectile and projectile kinetic energy at muzzle.

Relative position *S*	Muzzle velocity *v* (m/s)	Kinetic energy at muzzle *E* (J)
0	8.36	2.07
0.1	11.93	4.22
0.2	12.72	4.79
0.3	12.68	4.76
0.4	12.88	4.98
0.5	12.45	4.58
0.6	11.74	4.08
0.7	10.28	3.13
0.8	4.88	0.71
0.9	2.18	0.14

It can be found from Fig. 9 that the projectile kinetic energy at muzzle increases first and then decreases with the increase of the projectile's relative position. When the relative position of the projectile is between 0.4 and 0.5, its kinetic energy at muzzle reaches the maximum of about 4.98 J, when its velocity is 12.88 m/s. When half length of the projectile is put into the drive coil, its kinetic energy at muzzle reaches the maximum.

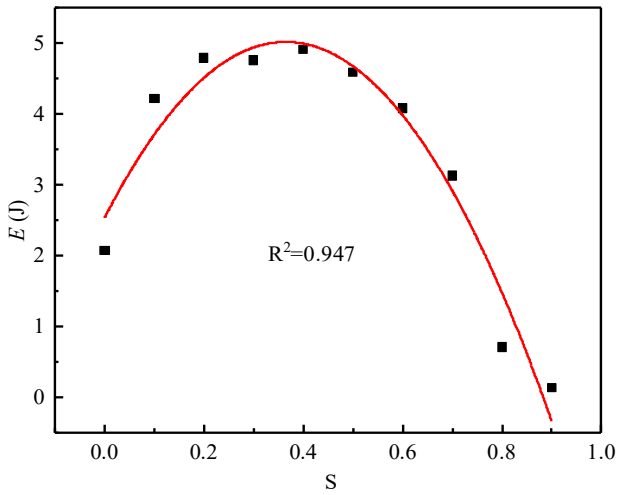

Fig. 9 Relationshop between relative position of projectile and projectile kinetic energy at muzzle.

4.5 Factors influencing projectile kinetic energy at muzzle

Based on the data of the relationship between the inductance, voltage, the capacitance and projectile position and the projectile kinetic energy at muzzle obtained from the above experiments, a multivariate nonlinear function program is established, and the fitting formula and parameter results are generated through MATLAB. The basic procedures are as follows.

The nlinfit function was used for nonlinear curve fitting, and the call format was beta=nlinfit(X, Y, fun, beta 0), where *X* and *Y* are lists of variables. The fun is the prototype and beta is the estimated initial value of each coefficient of the nonlinear function prototype. In addition, the beta is the calculated value corresponding to beta 0 [27].

The fitting results are:

$$\begin{aligned} y = &-10.646 + 0.579x_1 + 7.711\times10^{-3}x_2 + 5.153\times10^{-3}x_3 \\ &+17.454x_4 - 2.662\times10^{-2}x_1^2 - 6.456\times10^{-7}x_3^2 - 35.564x_4^2 \\ &+3.261\times10^{-4}x_1^3 - 1.624\times10^{-11}x_3^3 + 14.904x_4^3 \end{aligned} \quad (6)$$

where, the mean square error is 1.377.

Therefore, the relationship between the projectile kinetic energy E at muzzle and the coil inductance L, discharge voltage U, energy storage capacitance C and relative position S of the projectile is defined by the function below:

$$\begin{aligned} E = &-10.646 + 0.579L + 7.711\times10^{-3}U + 5.153\times10^{-3}C \\ &+17.454S - 2.662\times10^{-2}L^2 - 6.456\times10^{-7}C^2 - 35.564S^2 \\ &+3.261\times10^{-4}L^3 - 1.624\times10^{-11}C^3 + 14.904S^3 \end{aligned} \quad (7)$$

To verify the accuracy of Eq. (7), a coil gun experiment system with different specifications of drive coils and different discharge voltages was established. The parameters were as follows: coil inner diameter 17 mm, capacitance 2000 μF, projectile mass 0.6 kg, and projectile relative position 0.5.

The inductance values of the drive coils prepared using enamelled wire with different diameters were calculated. The launch process of the projectile was recorded by the high-speed camera, and its kinetic energy at muzzle was measured and compared with that obtained by the fitting formula, as shown in Table 7.

Table 7. Comparison between measured values of projectile kinetic energy at muzzle under different conditions and calculated values.

Inductance *L* (H)	Voltage *U* (V)	Measured energy *E* (J)	Calculated energy *E* (J)	Error (%)
2.40	700	4.34	4.79	9.39
3.37	700	4.80	5.21	7.86
7.86	700	5.98	6.61	9.53
10.65	700	6.42	7.09	9.45
13.67	700	6.66	7.32	9.01
16.24	700	6.62	7.33	9.68
20.65	700	6.37	7.03	9.38
4.18	600	4.28	4.75	9.89
4.18	500	3.65	3.98	8.29
4.18	400	2.99	3.21	6.85
4.18	300	2.20	2.44	9.83
4.18	200	1.53	1.67	8.38
4.18	100	0.82	0.90	8.88
2.40	700	4.34	4.79	9.39

As can be seen from Table 7, the error between the kinetic energy calculated by the fitting formula and the measured value is within 10%, indicating that the fitting formula is feasible when the voltage is 0-780 V and capacitance is 0-4800 μF. As seen from Figs. 10 and 11, the calculated values are slightly larger than the measured values, which is mainly due to the friction between the projectile and the inner wall of the gun tube, energy loss caused by coil temperature rise, and the error in velocity measurement.

The correlation analysis was conducted to measure the degree of linear correlation between variables, which was expressed by statistical indicators. The calculation algorithm in SPSS software defined the degree of correlation between different variables by calculating the correlation coefficient. The Pearson correlation coefficient *r* was used to calculate the correlation between continuous variables, and its value ranges from -1 to 1. The closer the absolute value of *r* is to 1, the higher the degree of correlation between the two variables [28, 29].

To study the influence degree of coil inductance, the energy storage capacitance, discharge voltage and the relative position of the projectile on the projectile kinetic energy at muzzle, and Pearson correlation coefficients were calculated by SPSS software, as shown in Table 8. It can be seen that the projectile kinetic energy at muzzle is significantly correlated with the energy storage capacitance and discharge voltage at the 0.01 level

Further analysis shows that the maximum correlation, 0.518, exits between the projectile kinetic energy at muzzle and the energy storage capacitance, and the minimum correlation, 0.17, exits between the projectile kinetic energy at muzzle and its relative position. Meanwhile, the correlation coefficients of the projectile kinetic energy at muzzle with the discharge voltage and the coil inductance were 0.442, 0.301, respectively.

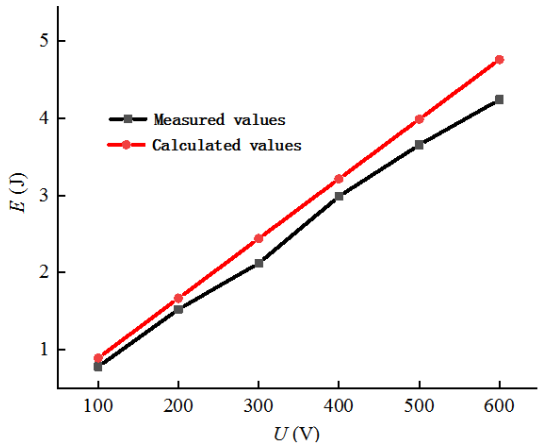

Fig. 10. Calculated and measured values of projectile kinetic energy at muzzle under different voltages.

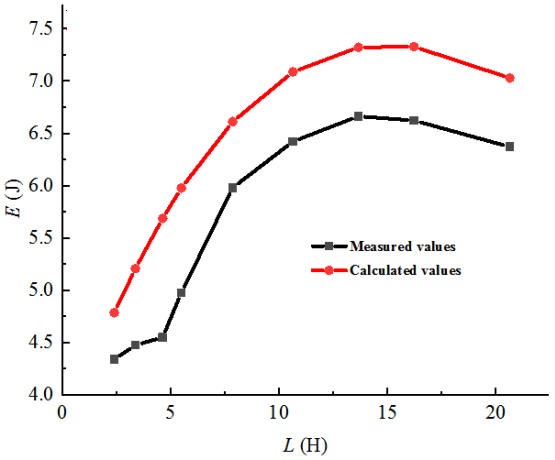

Fig. 11. Calculated and measured values of projectile kinetic energy at muzzle under different inductors.

Table 8. Correlation between variables.

Name		Inductance *L* (H)	Voltage *U* (V)	Capacitane *C* (uf)	Relative position *S*	Energy *E* (J)
Inductance *L* (H)	Pearson correlation	1	0.113	-0.109	0.028	0.301
	Sig. (two-tailed)		0.481	0.496	0.863	0.056
	Number of cases	41	41	41	41	41
Voltage *U* (V)	Pearson correlation	0.113	1	0.116	-0.029	.442**
	Sig. (two-tailed)	0.481		0.47	0.855	0.004
	Number of cases	41	41	41	41	41
Capacitance *C* (uf)	Pearson correlation	-0.109	0.116	1	0.028	.518**
	Sig. (two-tailed)	0.496	0.47		0.86	0.001
	Number of cases	41	41	41	41	41
Relative position *S*	Pearson correlation	0.028	-0.029	0.028	1	-0.17
	Sig. (two-tailed)	0.863	0.855	0.86		0.288
	Number of cases	41	41	41	41	41
Energy *E* (J)	Pearson correlation	0.301	.442**	.518**	-0.17	1
	Sig. (two-tailed)	0.056	0.004	0.001	0.288	
Note	** Correlation is significant at the 0.01 level (two-tailed).					

5. Conclusions

By using the self-made magnetoresistive coil gun, the relationship between the projectile kinetic energy at muzzle

and the coil inductance, discharge voltage, energy storage capacitance and relative position of the projectile was analyzed by changing the structure of the drive coil and the circuit component parameters, respectively. The main conclusions are obtained as following:

(1) The projectile kinetic energy at muzzle first increases and then decreases with the increase of coil inductance, increases linearly with voltage, increases first and then remains at a certain level with the increase of capacitance, and presents a quadratic function relationship with the position of the projectile.

(2) The relationship functions between the projectile kinetic energy at muzzle and the energy storage capacitor, discharge voltage, coil inductance, and relative position of the projectile were fitted. The sum of squared errors was 1.377, and the errors were all within 10% compared with the experimental results.

(3) The projectile kinetic energy at muzzle is significantly correlated with the energy storage capacitance and discharge voltage. The correlation coefficients of the kinetic energy with the energy storage capacitance, discharge voltage, coil inductance and relative position of the projectile were 0.518, 0.442, 0.301 and 0.17, respectively.

The coil gun can be combined with the SHPB device for dynamic loading tests under complicated stress conditions that involve both tensile and compressive stress, both compressive and shear stress, synchronous multiaxial stress and/or high-speed penetration. For being applied in the aerospace, underground and vehicle engineering and various civil works for dynamic mechanical performance tests on structural damage, material energy consumption, and mechanical collision [30-33], there are still a lot of works to be further studied.

Acknowledgements

This study was financially supported by the National Natural Science Foundation of China (41772163), and the Fundamental Research Funds for the Universities of Henan Province (NSFRF200202), China.

This is an Open Access article distributed under the terms of the Creative Commons Attribution License.

References

1. Wang, M., Chen, J. L., Cao, Y. J., "Muzzle velocity control method of synchronous induction coilgun". *Journal of Gun Launch & Control*, 35(1), 2014, pp. 1-5.
2. Fair, H. D., "Advances in electromagnetic launch science and technology and its applications". *IEEE Transactions on Magnetics*, 45(1), 2009, pp. 225-230.
3. Mcnab, I. R., "Progress on hypervelocity railgun research for launch to space". *IEEE Transactions on Magnetics*, 45(1), 2009, pp. 381-388.
4. Engel, T. G., Timpson, E. J., Veracka, M. J., "Demonstration of a reversible helical electromagnetic launcher and its use as an electronically programmable mechanical shock tester". *IEEE Transactions on Plasma Science*, 43(5), 2015, pp. 1266-1270.
5. Dutta, I., Delaney, L., Cleveland, B., Persad, C., Tang, F., "Electric-current-induced liquid Al deposition, reaction, and flow on Cu rails at rail-armature contacts in railguns". *IEEE Transactions on Magnetics*, 45(1), 2009, pp. 272-277.
6. Liu, W. B., Cao, C., Zhang, Y., Wang, J., Yang, D. W., "Parameters optimization of synchronous induction coilgun based on ant colony algorithm". *IEEE Transactions on Plasma Science*, 39(1), 2011, pp. 100-104.
7. Wang, S. R., Zhao, J. Q., Wu, X. G., Yang, J. H., Liu, A. "Meso-scale simulations of lightweight aggregate concrete under impact loading". *International Journal of Simulation Modelling*, 20(2), 2021, pp. 291-302.
8. Wu, X. G., Wang, S. R., Yang, J. H., Zhao, J. Q., Chang, X. "Damage characteristics and constitutive model of lightweight shale ceramsite concrete under static-dynamic loading". *Engineering Fracture Mechanics*, 259, 2022, pp. 108137.
9. Wang, G. Y., Wang, T. T., Wang, S. R., He, Y. S., Kong, F. L., Fan, J. Q. "Analysis of damage evolution characteristics of surrounding rock in deep anchorage cavern under dynamic loading". *Journal of Engineering Science and Technology Review*, 13(3), 2020, pp. 96-105.
10. Xiang, H. J., Lei, B., Yuan, X. C., "Mechanics and characteristics of induced current in armature for induction coil gun". *Journal of Artillery Launch and Control*, 38(4), 2017, pp. 1-5.
11. Liu, Z. S., Cheng, P. S., Wang, Z. R., "Close-range precise target design of coil gun based on PCHIP algorithm". *Manufacturing Automation*, 43(11), 2021, pp. 94-96.
12. Niu, X. B., An, Y. Z., Hu, Y. C., "Research on the temperature field distribution characteristics for thermal management of coilgun". *IEEE Transactions on Plasma Science,* 49(10), 2021, pp. 3193-3199.
13. Zhang, P. X., Shu, T., Shi, J. M., "Simulation analysis of asynchronous induction type coil gun armature structure parameters". *Journal of Physics: Conference Series*, 1939, 2021, pp. 012050.
14. Sejong, K., Jinho, K. "Optimal design of a coil gun projectile by analyzing the drag coefficient and electromagnetic force on the projectile". *Journal of Mechanical Science and Technology*, 34(7). 2020, pp. 2903-2911.
15. Guo, W., Su, Z. Z., "Muzzle velocity and efficiency performance of single-stage induction coilgun". *Journal of Artillery Launch and Control*, 37(2), 2016, pp. 1-4.
16. Orbach, Y., Oren, M., Golan, A, Einat, M., "Reluctance Launcher Coil-Gun Simulations and Experiment". *IEEE Transactions on Plasma Science*, 47(2), 2019, pp. 1358-1363.
17. Wang, Y., Lin, F. C., "Design and analysis of driving coil in induction coil gun". *Journal of Huazhong University of Science and Technology (Natural Science Edition)*, 50(1), 2022, pp. 26-30.
18. Guan, X. C., Lei, B., "Field circuit and movement coupled time stepping finite element analysis on single-Stage inductive coil gun". *Transactions of China Electrotechnical Society*, 26(9), 2011, pp. 138-143.
19. Guo, D. H., Shi, D. L., "Simplification of capacitance driven multistage coilgun model". *Electric Machines and Control*, 26(5), 2022, pp. 8-16.
20. Kim, S., Kim, J., "Optimal design of a coil gun projectile by analyzing the drag coefficient and electromagnetic force on the projectile". *Journal of Mechanical Science and Technology*, 34(7), 2020, pp. 2903-2911.
21. Coramik, M., Citak, H., Bicakci, S., Gunes, H., Aydin, Y., Ege, Y., "Studies to increase barrel exit velocity for four-stage coil-gun". *IEEE Transactions on Plasma Science*, 48(7), 2020, pp. 2618-2627.
22. He, Y. H., Wang, Y., "A new structure of linear rotating accelerated coilgun". *Acta Armamentarii*, 39(9), 2018, pp. 1858-1863.
23. Ranashree, R., Thomas, M. J., "Experimental and computational studies on the efficiency of an induction coilgun". *IEEE Transactions on Plasma Science*, 48(10), 2020, pp. 3392-3400.
24. Xiang, H. J., Li, Z. Y., Lei, B., "Analysis on interior ballistics of multi-stage inductive coil gun based on coupling of field and circuit". *Journal of Ballistics*, 24(3), 2012, pp. 100-104.
25. Zou, B. G., Sun, X. F., "Scale model and model experiment of electromagnetic coil launcher". *Transactions of China Electrotechnical Society*, 28(2), 2013, pp. 73-77.
26. Wu, S. W., "Inductance tables of air-cored cylindrical coil". *Journal of Zhengzhou University (Engineering Science)*, (3), 2003, pp. 106-112.

27. Gao, C., "Program implementation and optimization of surface subsidence predicting parameters determination based on Matlab curves fitting". *Coal Mining Technology*, 23(1), 2018, pp. 33-37.
28. Zhao, X. J., Liang, Z. D., Shao L. J., Zhao, X. F., "A new weighted mixed two-parameter estimator under stochastic constraints". *Statistics & Decision*, 37(23), 2021, pp. 20-22.
29. Luo, Z. M., Kang, K., "Correlation analysis and regression model of multiple explosive gas based on SPSS". *Coal Technology*, 35(1), 2016, pp. 157-160.
30. Wang, S. R., Shi, K. P., Zou, Y. F., Zou, Z. S., Wang, X. C., Li, C. L. "Size effect analysis of scale test model for high-speed railway foundation under dynamic loading condition". *Tehnicki Vjesnik-Technical Gazette*, 28(5), 2021, pp. 1615-1625.
31. Chang, X., Wang, S.R., Li, Z., Chang, F. G. "Cracking behavior of concrete/rock bi-material specimens containing a parallel flaw pair under compression". *Construction and Building Materials*, 360, 2022, pp. 129440
32. Wang, S. R., Wang, Z. L., Gong, J., Wang, Y. H., Huang, Q. X. "Coupling effect analysis of tension and reverse torque during axial tensile test of anchor cable". *DYNA*, 95(3), 2020, pp. 288-293.
33. Glavaš, B., Peršec, Z. "Technical aspects of lithotripters and application of shock wave therapy ESWL in the treatment of urinary tract stones". *Technical Journal*, 8(2), 2014, pp. 145-149.